A Physicochemical Approach to Interpret the Biological Activities of some Dipeptide Systems

[1]KH. M.E. HASHEM, F.A-E-A. ALI AND [2]M.A.T. IBRHAIM
[1]*Chemistry Department, Faculty of Science, Ain-Shams University Cairo, Egypt*
[2]*Applied Maths Department, Faculty of Science, Ain-Shams University, Cairo Egypt*

(Received 25th October, 1997, revised 17th September, 1998)

Summary: The biological activities for four-Iso-nicotinoyl dipepetide systems are attributed to some physiochemical parameters. The semi-empirical MNDO together with the AMI methods, were applied to define these parameters by optimizing the structural energy of the four systems with respect to incremental variation of their backbone dihedral angles. The lowest energetic structures are determined by generating two ECD maps by plotting $\phi^1 1$ vs $\Psi^1 1$ and $\Psi^1 1$ vs $\phi^2 1$ dihedral angles for each of the four systems. The comparison between the lowest energetic structures reveals that these systems have permanent dipole moments. Based on the different susceptibilities of the dipeptide tails to rotate as bonded charged masses around the X-axis of the molecular frame, the Gaussian cylinders characteristic by nine different charged zones could be speculated. The sign of the residual charges on the zones corresponding to the backbone's bonds and side chain residues, which are labelled section 2, are defined as the required physicochemical parameters. It appears that the biological activity of each system is affected by the sign of the charges allocated on the above section of each system. If the charge is +ve then the corresponding dipeptide system(s) should posses biological activities, otherwise the system(s) are biologically inactive.

Introduction

The identification of the primary structure, of a peptide via a specific structural parameter which was selected from the ^{13}C-NMR spectrum for 28 common amino acids, was the target of the previous work [1]. One of the current problems is the investigation of the relationships between the secondary structure and biological function of a peptide [2]. A set of peptides could be selected as a representative model [3], if the following criteria are achieved; (1). The peptides have structural similarity, (2). The peptides possess different biological affinities. A set of four simple dipeptides, named iso-nicotinoyl-Lx_1-Lx_2 methyl ester, was selected from the literature to be a model [4] for the present study. Their structures are classified to head and tail. Hereafter, the four dipeptides are called **a**,**b**,**c** and **d**, where:

Dipeptide symbol (monomer)	Head	1st amino acid Lx_1	2nd amino acid Lx_2	End Group EG
a	iso-nicotinoyl	valine	valine	methyl ester
b	iso-nicotinoyl	valine	leucine	methyl ester
c	iso-nicotinoyl	valine	serine	methyl ester
d	iso-nicotinoyl	valine	tyrosine	methyl ester

The dipeptides **b** and **d** actually possess biological activities towards *Pseudomonas aeruginose, Candida utilis, Candida albicans* and *Spergillus niger* [4]. While dipeptides **a** and **c** are biologically inactive towards the same organisms [4].

The main target of the present study is to determine the physicochemical parameters(s) upon which the variation of their biological activities could be interpreted.

Procedure

(I) Staring geometries

The four extended structures of the dipeptide systems are shown in Fig. 1- (a-d). The atoms' type scheme and symbolic nomenelature are listed in Table-1. The extended structures are partitionated to head (nicotinoyl nucleus), tail (dipepetide amino acids) and end group (methyl ester) (1). The structure of the nicotinoyl moiety is planar with fixed bond lengths and angles [5]. The Cartesian origin of the molecular frame was fixed to coincide with $C'_{[4]}$ while the X-axis was aligned with $C'_{[4]}$--$C^*_{[7]}$ bond (2). The initial secondary structures of the first and second amino acids of the four tails were pertained as previously published [6] (3). Due to the uncertainties in the position of the hydrogen atoms, they are neglected from the numbering system (4). The tetrahedral angles of the terminal methyl of the

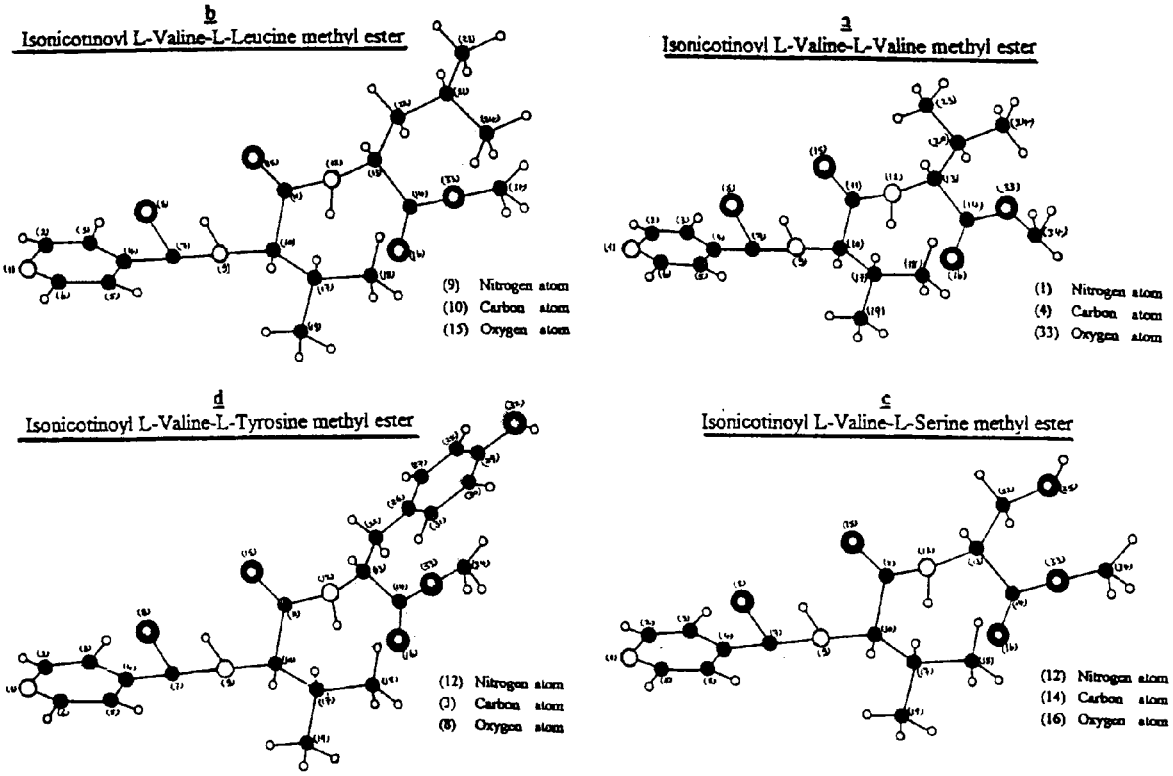

Fig. 1: Extended sructures of the four dipeptide monomers.

end group is assumed typical. The nonhydrogen atoms of the end group are not considered as backbone atoms (5). Rotation of the dipeptide tail around and X-axis was the only rotational motion considered (6). Although, the peptide groups have their own planar structures due to the localized resonance, yet, the co-planarity between them in each system was not achieved.

(II) Molecular potential energy

(A) Intramolecular potential energy

The calculated electrostatic pairwise, repulsive nonbonded types 1-4 and 1-5 and hydrogen bond interactions are summed for each new generated isomer to evaluate its intramolecular potential energy [7]. To reduce the computational time during the calculation of the intramolecular potential energy, the following selection rules are applied (1). During the calculation of electrostatic pairwise interaction, cut off distances greater than 12A° are imposed (2). For repulsive nonbonded 1-4 and 1-5 interactions, distances greater then Van Der Waal's radii plus 4A° are rejected (3). Torsional energies associated with rotation around the partial π-bond(s) are not considered.

(B) Intermolecular potential energy

Based on the polarizabilities of the four dipepetide systems, the intermolecular potential energies, in terms of London attraction dipole-dipole energies, are explored. The following selection rules are applied during the calculations (1). The length of each dipeptide tail (R), is defined as the sum of bond lengths between N2 [9] atom of the first amino acid and the furthest atom of the second amino acid plus the Van Der Waals radius of the furthest atom (2). London attraction energy is itteratively calculated within the bounded range of (R to R+4A°) by using

the inverse sixth power of R assuming that the temperature is constant (3). When the distance between two monomers is very large, induce-dipole induce-dipole interaction energies are calculated by using two point charge vectors.

(III) Sequence of computational analysis

Assuming that each iso-nicotinoyl dipeptide molecule exists in a monomer state. Two optimization cycles are designed to generate numerous structural transitions by varying the values of $\phi^1 1$ vs $\Psi^1 1$ and $\Psi^1 1$ vs $\phi^2 1$ backbone dihedral angles. The Ist optimization cycle for the four dipeptide systems is initiated when $C^*_{[10]}$--$C^*_{[11]}$ bond lies in or parallel to the X-Y plane of the molecular frame. For each structural variation, the partial charges on the hydrogen and nonhydrogen atoms, are computed by applying the semi-empirical molecular orbital methods named Minimum Neglect of Differential Overlap "MNDO" and Austin Model 1 "AMI", to evaluate the molecular potential energy of the generated isomer [8-15]. The values of the backbone dihedral angle $\phi^1 1$ an $\psi^1 1$ at which the lowest energetic structures are achieved, is the criteria by which the first optimization cycle was terminated. On the basis of Van Der Waal's radii and triangle sum rules [16], a set of constraints was proposed to select one of the generated structures as a starting geometry for the second optimization cycle.

The initiation of the second optimization cycle is conditioned by (1). The optimized value of $\phi^1 1$ dihedral angle is kept constant from the first cycle (2). The corresponding value of $\psi^1 1$ was introduced as initial input in a nested do loop with the full incremental scale of $\phi^2 1$. The second optimization cycle was terminated by determining new values for $\psi^1 1$ and $\phi^2 1$ which produce the lowest energetic structure. At the end of each optimization cycle the sum of the computed intra- and intermolecular potential energies for each generated structure, were plotted in the form of Energy Contour Diagrams (ECD).

IV Determination of the charge densities on the gaussian cylinder's surfaces

The four dipeptide tails are treated as non-vibrational bonded systems which freely rotate around the X-axis to produce Gaussian cylinders after a whole rotation cycle [17]. The densities of the formed charges on the surface of the Gaussian cylinders' of each tail are calculated on the basis of the charge per unit area (λ/A^{o2}), cylinder radius (rA^o) and cylinder length (LA^o). The produced Gaussian cylinders' surfaces of the different tails are divided into nine fixed zones named in order $\theta^1 1$, $\theta^2 1$. $\phi^1 1$, $\psi^1 1$, $\omega^1 1$, $\phi^2 1$, $\psi^2 1$, $\omega^2 1$ and EG. The charges on the nine zones are divided into three sections. Sections **1** and **3** represent zones **1** and **9** respectively. While section **2** includes the zones from **2** to **8**.

Results and Discussion

Type, number and length of each bond in the structures of the four dipepetide systems are listed in

Table-1: The one atom type scheme and symbolic nomenclature of each type

	Carbon(C)		Nitron(N)		Hydrogen(H)		Oxygen(O)
Symbols	Chaacters	Symbols	Chaacters	Symbols	Characters	Symbols	Characters
C2	sp^3 Carbon with two H	N^*	sp^2 Nitrogen in six member ring with lone pair	$H^\backslash$	Hydrogen attached with carbon	$O^\backslash$	Carbonyl oxygen
C3	sp^3 Carbon with three H			H^*	Hydrogen attached with nitrogen	O^e	Ester oxygen
CA	sp^2 Aromatic carbon in six member ring with one H	N2	sp^2 Nitrogen attached with carbonyl group	H	Hydrogen attached with oxygen	O^h	Alcohol oxygen
C*	sp^3 Carbon with one H						
C	sp^2 Aromatic carbon in six member ring with one substituent						
C*	sp^2 Carbonyl carbon and aromatic carbon with hydroxyl substituent in tyrosine						

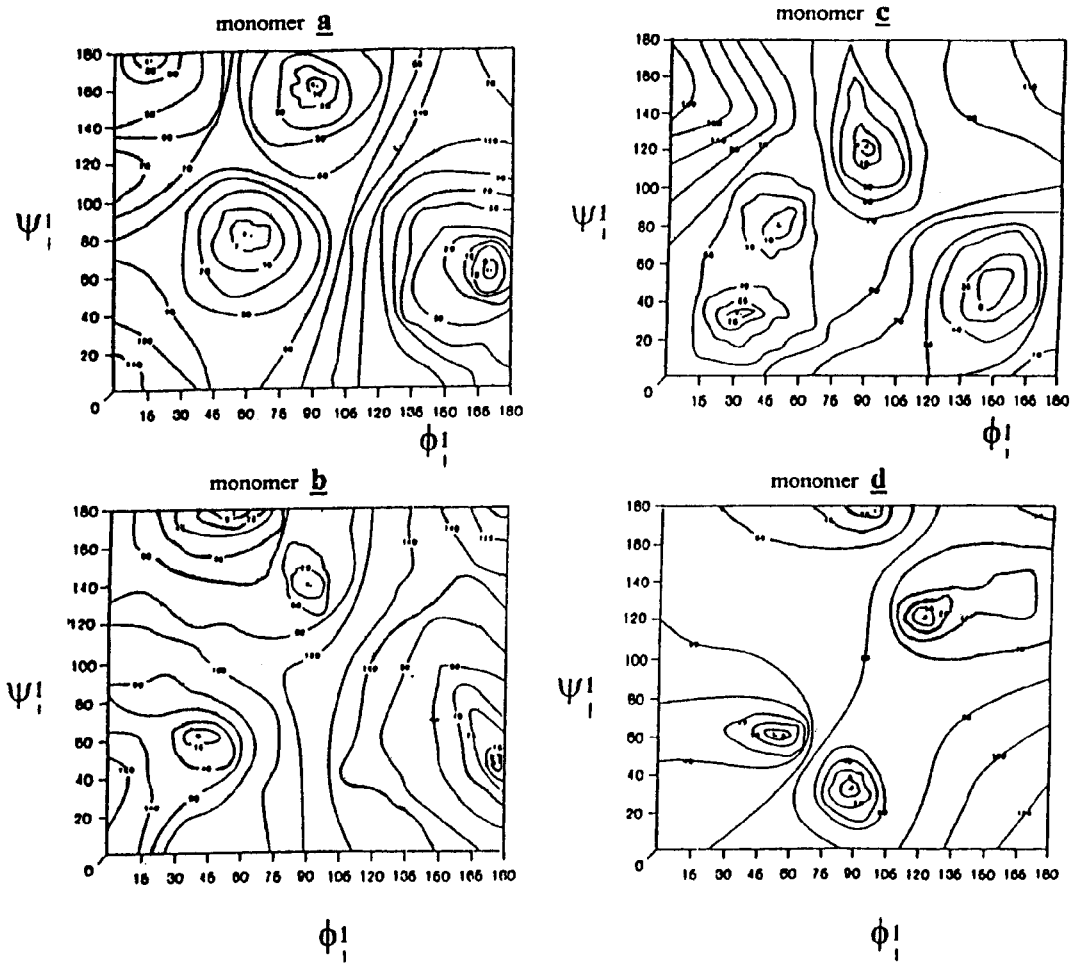

Fig. 2a: Energy contour diagrams (ECD) at the end of the Ist optimization cycle to optimize $\psi^1 1$ vs $\phi^1 1$

Table-2. The ECD maps of the **a,b,c**, and **d** dipeptide systems at the end of the first optimization cycle are plotted in Fig. 2a. Each ECD map includes four lowest minima, however, this phenomenon supports the similarity between the structures of the four optimized dipeptide systems. The lowest energetic structures deduced from the ECD maps are;$\phi^1 1 = 170°$, $\psi^1 1 = 65°$; $\phi^1 1 = 175°$, $\psi^1 1 = 50°$; $\phi^1 1 = 150°$, $\psi^1 1 = 48°$ and $\phi^1 1 = 60°$, $\psi^1 1 = 60°$ for **a,b,c** and **d** dipeptide systems ψrespectively. Although, the a-helical structure can not exist in a simple dipeptide molecule, however, the appearance of a low energetic conformer at $\phi^1 1 = 60°$ and $\psi^1 1 = 60°$ for system d nominating the existance of a low helical structure due to the phenolic ring of tyrosine [18]. However, it has been noticed that the value of the highest computed energies within the first optimization cycle over all the systems are above 140 Kcal/mole.

Table-3 shows the optimized values of the structural parameters $\psi^1 1$ and $\phi^2 1$ backbone dihedral angles at the end of the 2nd optimization cycle. The lowest energetic structures for **a,b,c** and **d** monomers are spotted at $\psi^1 1 = 70°$, $\phi^2 1 = 160°$; $\psi^1 1 = 60°$, $\phi^2 1$ 60°; $\psi^1 1 = 90°$, $\phi^2 1 = 90°$; $\psi^1 1 = 85°$, $\phi^2 1 = 95°$ respectively. The number of energy minima for monomers **a,b,c** and **d** are 3,2,3 and 2 respectively. The values of the highest computed energies at the end of the 2nd optimization cycle were computed as 90, 120, 75 and 120 Kcal/mole for **a,b,c** and **d** monomers, respectively. The depressions of these

Table-2: Number and types of bonds and their lengths in respect to the one atom scheme

Symbols	C3-C2	C2-C$^{\alpha}$	C$^{\backslash}$-C$^{\backslash}$	C$^{\backslash}$-C$^{\alpha}$	C2-CA	C$^{\alpha}$-C$^{\alpha}$	C$^{\alpha}$-C$^{\alpha}$	C3-H	C2-H$^{\backslash}$	CA-H$^{\backslash}$	C$^{\backslash}$-N$^{\alpha}$
Bond length A°	1.53	1.47	1.42	1.53	1.53	1.53	1.53	1.09	1	1.09	1.297
a	4	-	4	1	-	2	2	5	-	-	1
b	4	2	4	1	-	1	2	5	1	-	1
c	2	1	4	1	-	1	2	3	1	-	1
d	2	1	4	1	1	1	2	3	1	4	1

Symbols	C$^{\alpha}$-N2	C$^{\alpha}$-N2	C$^{\alpha}$-O$^{\backslash}$	C$^{\alpha}$-O^{h}	C3-O^{h}	CA-O^{h}	N^{2}-H$^{\alpha}$	O^{h}-H	CA-CA	C$^{\backslash}$-H$^{\backslash}$	C2-O^{H}
Bond length A°	1.469	1.325	1.23	1.35	1.425	1.36	1.014	0.96	1.42	1.085	1.312
a	2	2	3	1	1	-	2	-	-	4	-
b	2	2	3	1	1	-	2	-	-	4	-
c	2	2	3	1	1	-	2	1	-	4	1
d	2	2	3	1	1	1	2	1	6	4	-

Table-3: Results of the second optimization cycle by varing $\psi^1 1$ vs. $\phi^2 1$ using semi-empirical MNDO together with AM1 methods.

	Configuration of the Energy Minima Regions											
Amino Acid			1		2				3			
			Enegy Kcal/mol$^{\alpha}$				Enegy Kcal/mol$^{\alpha}$				Enegy Kcal/mol$^{\alpha}$	
Residues	$\psi^1 1$	$\phi^2 1$	Min	Max	$\psi^1 1$	$\phi^2 1$	Min	Max	$\psi^1 1$	$\phi^2 1$	Min	Max
(a) Val-Val	70	160	0	90	170	15	2.4	90	120	95	5.4	90
(b) Val-Leu	60	60	0	120	149	155	6.7	120	-	-	-	-
(c) Val-Ser	90	90	0	75	130	40	2.9	75	115	140	7.5	75
(d) Val-Tyr	85	95	0	120	150	85	7.5	120	-	-	-	-

N.B: The energies are in units of Kcal/mole relative to zero at the lowest energy minimum

Physico-chemical Parameter	Type of Overlap	Monomers	Real Biological Status	Charge distribution Head	1	Tail 2	3	Electron Distribution Overlap
				+ve	-ve	-ve	-ve	
-ve	Constructive	**a & c**	Inactive	+	-	-	-	Continuous
			No local electrostatic sites					
				+ve	-ve	+ve	-ve	
+ve	Destructive	**b&d**	Active	+	-	+	-	Discrete
			Local electrostatic sites					

final optimized values of the maximum energies than that firstly optimized are 50, 20, 65 and 20 Kcal/mole for **a, b, c,** and **d** systems respectively. These depressions indicated that; (1) The capability of 2nd optimization cycle, to refine the optimum dipeptide structures of the first cycle (2). The a-helical structure of b system could be confirmed, where the final refined values of both $\psi^1 1$ and $\phi^2 1$ dihedral angles are equal to 60° (3). The energies of the optimized structures and number of energy minima, after the second optimization cycle, of monomers **b** and **d** are similar to each other, but differ than monomers **a** and **c,** which are also similar. Fig. 2B declares the ECD's of the 2nd optimization cycle to optimize $\psi^1 1$ vs. $\phi^2 1$.

Table-4 indicates the final set of the computed partial charges on the hydrogen and nonhydrogen atoms of the four dipeptide systems, from which the lowest potential energies corresponding to the optimum values of ψ's and ϕ's dihedral angels are calculated. The following remarks were deduced from the computed partial charges;

(i) The $C2_{[22]}$ of leucine and tyrosine side chain of **b** and **d** molecules have partial charges -

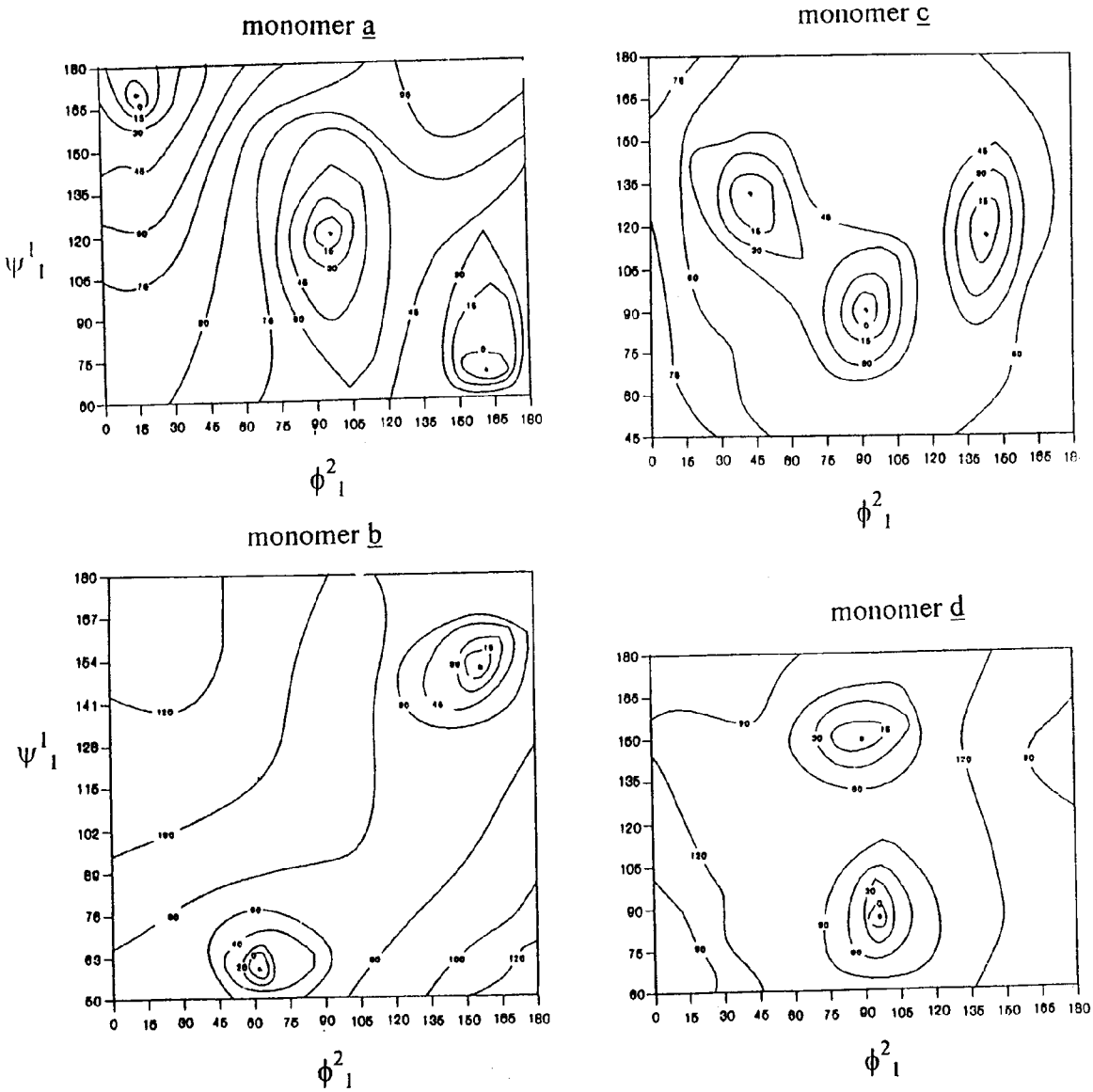

Fig. 2b: Energy contour diagrams (ECD) at the end of the 2nd optimization cycle to optimize $\psi^1 1$ vs $\phi^2 1$

0.033 and -0.05 ecu respectively, while the same atom of serine in molecule **c** exhibits positive partial charges +0.139 ecu. So, the partial charge on C_β atom of saturated side chain reflects the polarity on the subsequent atoms' being slightly negative if C_γ atom is carbon and becomes positive if C_γ is oxygen.

(ii) The net partial charges on $C'_{[2]}$, $C'_{[3]}$ and $C'_{[4]}$ were computed as -0.058, -0.132 and -0.075 ecu respectively. These values are in full agreement with the resonance rule on pyridine ring. However, the polarity of the nicotinoyl head could be attributed to the separate contributions of both localized resonance on pyridine ring and -C-N-C moiety.

(iii) The constancy of the calculated partial charges's values, on the hydrogen and non-hydrogen atoms of the first amino acid of all systems, indicate

Table-4: The Computed Charge Distributions for the Final Optimized Structures which are Calculated by MNDO together with AMI methods

No. of Atom	Classification	Type of Atoms	Charge Distribution												No. of attached hydrogen atoms
			Charge distribution over the nonhydrogen atoms				Charge on the attached hydrogen atoms				Net partial charge on the nonhydrogen atoms				
			a	b	c	d	a	b	c	d	a	b	c	d	
1		N	-516	-516	-516	-516	-	-	-	-	-516	-516	-516	-516	-
2		C$^{\backslash}$	-123	-123	-123	-123	65	65	65	65	-58	-58	-58	-58	1
3	Pyridin	C$^{\backslash}$	-155	-155	-155	-155	23	23	23	23	-132	-132	-132	-132	1
4	ring	C$^{\backslash}$	-75	-75	-75	-75	-	-	-	-	-75	-75	-75	-75	-
5		C$^{\backslash}$	-155	-155	-155	-155	23	23	23	23	-132	-132	-132	-132	1
6		C$^{\backslash}$	-123	-123	-123	-123	65	65	65	65	-58	-58	-58	-58	1
7	Carbonyl	C$^{\backslash}$	470	470	470	470	-	-	-	-	470	470	470	470	-
8	group	O$^{\backslash}$	-413	-413	-413	-413	-	-	-	-	-413	-413	-413	-413	-
9		N2	-495	-495	-495	-495	165	165	165	165	-330	-330	-330	-330	1
10		C*	81	81	81	81	30	30	30	30	111	111	111	111	1
11	Back	C*	410	410	410	410	-	-	-	-	410	410	410	410	-
12	bone	N2	-431	-431	-431	-431	145	145	145	145	-286	-286	-286	-286	1
13		C*	72	72	72	72	29	29	29	29	101	101	101	101	1
14		C*	425	425	425	425	-	-	-	-	425	425	425	425	-
15	Carbonyl	O$^{\backslash}$	-430	-430	-430	-430	-	-	-	-	-430	-430	-430	-430	-
16	oxygen	O$^{\backslash}$	-427	-427	-427	-427	-	-	-	-	-427	-427	-427	-427	-
17	First amino	C*	8	8	8	8	16	16	16	16	24	24	24	24	1
18	acid	C3	-72	-72	-72	-72	75	75	75	75	3	3	3	3	3
19	side chain	C3	-72	-72	-72	-72	75	75	75	75	3	3	3	3	3
20		C*	8	-	-	-	16	-	-	-	24	-	-	-	1
21		C*	-	14	-	-	-	24	-	-	-	10	-	-	1
22		C2	-	-33	139	-50	-	54	44	36	-	21	183	-14	2
23		C3	-72	-75	-	-	75	69	-	-	3	-6	-	-	3
24	Second	C3	-72	-75	-	-	75	69	-	-	3	-6	-	-	3
25	amino	O^{h}	-	-	-350	-	-	-	107	-	-	-	-17	-	1
26	acid	CA	-	-	-	35	-	-	-	-	-	-	-	35	-
27	side chain	CA	-	-	-	-9	-	-	-	14	-	-	-	5	1
28	chain	CA	-	-	-	-45	-	-	-	28	-	-	-	-17	1
29		CA	-	-	-	212	-	-	-	-	-	-	-	212	1
30		CA	-	-	-	-45	-	-	-	28	-	-	-	-17	1
31		CA	-	-	-	-9	-	-	-	14	-	-	-	5	1
32		O^{h}	-	-	-	-310	-	-	-	135	-	-	-	-175	1
33	End	O^{e}	-375	-375	-375	-375	-	-	-	-	-375	-375	-375	-375	-
34	Group	C3	-85	-85	-85	-88	78	78	78	78	-7	-7	-7	-7	3

N.B: 1. The located charges must be divided by 10^3 to be in ECU (Electron Charge Unit).
2. The represented charges on all heavy atoms don't include the hydrogen charges.
3. The calculated net charge is the algebric sum of the charges on the central atom and its attached hydroge proto

e-5: Parameters and charge densities on the Gaussian cylinders' zones for all monomers

Code Number			1	2	3	4	5	6	7	8	9
omer Gaussian Parameters			Charge densities over Gaussian cylinder's zones in ecu/A^2 units**								
ols L A°	R A°	Av.ecu/A^2	C*(7)-O'(8)	N2(9)--C*(10)	C*(10)-C*(11)	C*(11)-O'(15)	1st side	N2(12)-C*(13)	C*(13)-C*(14)	2nd side	O'(33)-C
10.82	4.38	-0.158	-1.3396	-0.3133	0.0984	-0.017	0.221	-0.537	0.1435	0.3313	-0.2462
1.46	4.86	-0.132	-1.6452	-0.3039	0.0996	-0.009	0.231	-0.542	0.1749	0.5752	-0.2731
9.21	3.91	-0.186	-1.1751	-0.3729	0.0932	-0.026	0.268	-0.578	0.1363	0.3399	-0.3528
3.09	5.34	-0.116	-1.8317	-0.3935	0.0988	-0.0221	0.296	-0.551	0.1962	0.8171	-0.2915
Standard Deviation			0.2957355	0.04405118	0.002909754	0.007341832	0.03453501	0.018275667	0.027908705	0.23042793	0.045265

table-4 net charge distribution on each central atom.
e charge density of each zone is calculated as an individual cylinder according to the Gaussian principles.

that the polarizability of the iso-nicotinoyl head does not extend to the amino acids of each tail.

Table-5 shows the computed values of the Gaussian parameters (L, r and λ/A°2) and the nine defined charged zones of each system. The following remarks have been noticed;

(i) The negative charges were resident on zones corresponding to the projections of the backbone's bonds only. These bonds are $C^{*}_{[7]}$--$O'_{[8]}$, $N2_{[9]}$--$C^{*}_{[10]}$, $C^{*}_{[11]}$--$O'_{[15]}$, $N2_{[12]}$--$C^{*}_{[13]}$ and $Oe_{[33]}$--$C3_{[34]}$. However, the differences between the similar computed values of these negative charges overall the four dipeptide monomers are due to the variation in the physical parameters of the Gaussian cylinders.

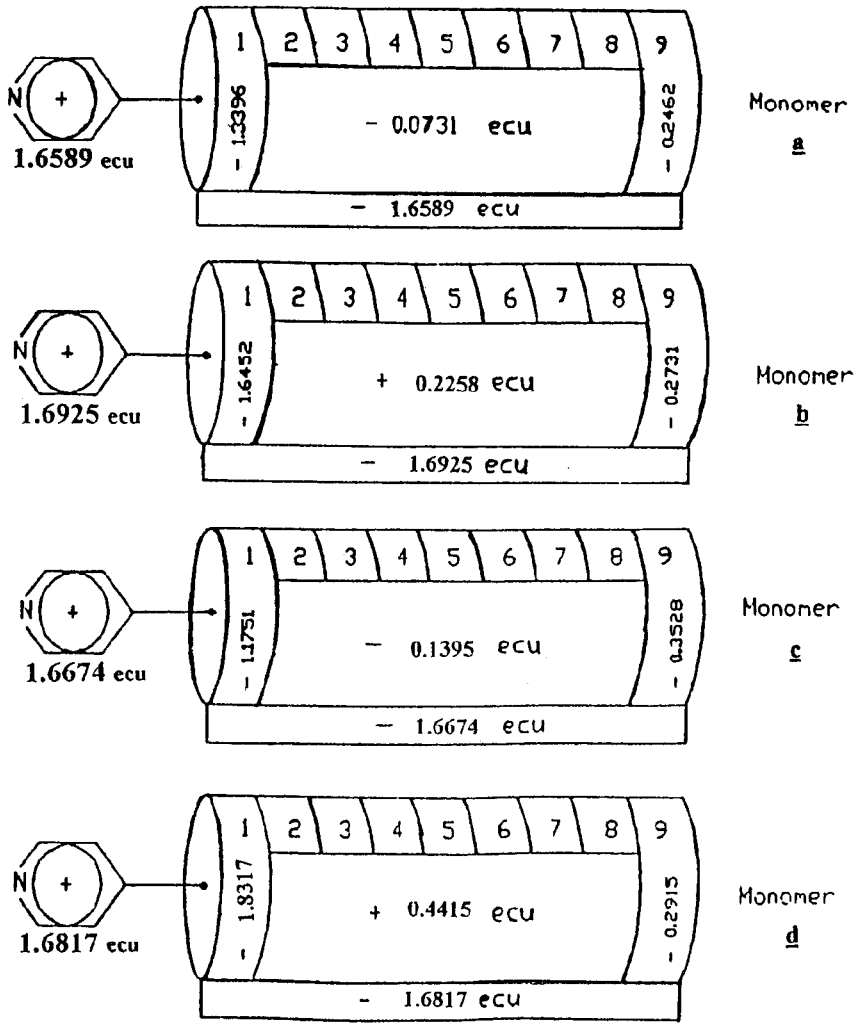

Fig. 3: A Schematic diagram that indicates the charge distribution on the Gaussian cylinders' surfaces for all monomers.

(ii) The positive charges accommodated on the projections of $C^{*}_{[10]}$--$C^{*}_{[11]}$, side chain of the first amino acid, $C^{*}_{[13]}$--$C^{*}_{[14]}$ and second amino acid side chain bonds. The more dense positive charges on the zone $C^{*}_{[13]}$--$C^{*}_{[14]}$ rather than then zone $C^{*}_{[10]}$--$C^{*}_{[11]}$ in the systems are attributed to the polarity of the vicinal oxygen atoms $Oe_{[33]}$.

Fig. 3 is a schematic diagram that indicates the distribution of the calculated residual charges on the nine zones of the Gaussian cylinder's surfaces of the four dipeptide systems. The correlation study between the three sections of the four Gaussian cylinders reveals that; (1). The algebric sums of the residual charges, over all three sections of each Gaussian cylinder's surface, for the four systems, have approximately equal numerical negative values within ± 0.0168 ecu. This result ensures the structural similarity between the four optimized monomers (2). The four dipeptide monomers are classified as polar molecules, since their most stable lowest energetic structures exhibit two opposite charges. Quite often, these two opposite charges (+ve located on the head and -ve located in the center of the tail) must be equal to achieve the molecular

neutrality. The existence of these two permanent opposite charges constitute a dipole moment. Average dipole moment per unit volume can be regarded as the charge per unit area "polarization". On the basis of the values of the calculated polarization ecu/A° (cf. Table-5), the four dipeptide molecules are arranged in the following order **c** > **a** > **b** > **d** (3). The four dipeptides could be classified to two groups according to the sequential order of the sign of the permanent charge on the head and three sections of each tail. The characteristics sequence of the charge sign of the first group is a +ve charge on the head and continuous -ve charges on the tails's three sections. Monomers **a** and **c** belong to this group, while they actually exhibit biologically inactive properties. Monomers **b** and **d** actually exhibited active biological properties, while they were found to belong to the second group which is characterized by a discrete charge sequence as +ve, -ve, +ve and -ve, on the head and the tail's sections, respectively.

Conclusion

The formation of either continuous or discrete residual charge types, on the heads and the tails' three sections, of monomers (**a** and **c**) and monomers (**b** and **d**), could cause constructive and destructive types of electron distribution overlaps, respectively. These overlaps are represented in the following table;

One can conclude that the type of the charge on section 2, is the only physicochemical parameter which controls the type of the electron distribution overlap and generates local electrostatic sites on the Gaussian cylinder surfaces.

(a) If the physicochemical parameter is -ve

No local electrostatic sites are generated. So, one can deduce that the dipeptide(s) inhibition interaction abilities, towards the mentioned organism(s), is inversely proportional to the number of electrostatic sites [19]. Therefore, the biological inactive property is domain.

(b) If the physicochemical parameter is +ve

It could be speculated that the formation of local electrostatic sites on the tail's section of backbone and side chain residues, could cause local-structure-disrupting of the covalency properties of the side chain bonds [11]. The process could separate a simple product, on which the organisms' growth might accelerate. Therefore, the biological active property is domain.

Finally, the type of the charges on section 2 of the Gaussian cylinder of the dipeptide tail, is the only physicochemical parameter suitable, to interpret the status of the biological activities of the four introduced dipeptide systems.

References

1. Kh.M.E. Hashem and F.A.E. Ali, *Bull. Soc. Chim. Belg.*, **94**, 735 (1985).
2. D, Wen and R.A. Laursen, *J. Biol Chem.*, **268**(22), 16401 (1993).
3. S.S. Vishveshwara and S.W. Vishveshwara, *Biophys. Chem.*, **46**(1), 77 (1993).
4. A.M. El-Naggar, M.E. Hussein, E.M. El-Nemma and A.A. Sammour, *Farmaco Ed. Sci.*, **40**(9), 662 (1985).
5. Tabnles of intratomic distances and configuration molecules and ions. The Chemical Society of London, 1956-1959.
6. F.A. Momany, R.F. McGuire, A.W. Burgess and H.A. Scheraga, *J. Phy. Chem.*, **79**(22), 2361 (1975).
7. S.R. Wilson, W. Cui, J.W. Moscowitz and K.E. Schmidt, *Tetrahedron Lett.*, **29**, 4373 (1988).
8. M.J.S. Dewar, W. Thiel, *J. Am. Chem. Soc.*, **99**, 4899 (1977).
9. M.J.S. Dewar, W. Thiel, *J. Am. Chem. Soc.*, **100**, 784 (1978).
10. M.J.S. Dewar, E.G. Zoebisch, E.F. Haley and J.J.P. Steward, *J. Am. Chem. Soc.*, **107**, 3902 (1985).
11. J.J.P. Steward, *J. Comp. Chem.*, **10**, 209 (1989).
12. K. Korzekwa, W. Trager, M. Gouterman, D. Spangler and G.H. Loew, *J. Am. Chem. Soc.*, **107**, 4273 (1985).
13. A. Goldblum and G.H. Loew, *J. Am. Chem. Soc.*, **107**, 4265 (1985).
14. M.J.S. Dewar and H.S. Rzepa, *J. Am. Chem. Soc.*, **100**, 58 (1978).
15. M.J.S. Dewar and H.S. Rzepa, *J. Am. Chem. Soc.*, **100**, 784 (1978).
16. T.F. Havel, I.D. Kuntz and G.M. Crippen, *Bull. Math. Biol.*, **45**, 665 (1983).

17. F.W. Sears, M.W. Zemansky and H.D. Young, College Physcs, fifth edition, ADDISON-WESLEY Publishing Company, Reading, p. 443 (1980).
18. R. Bessalle, A. Gorea, I. Shalit, J.W. Metzger, C. Dass, D.M. Desiderio and M. Fridkin, *J. Med. Chem.*, **36**(9), 1203 (1993).
19. J.L. Fauchere, M. Charton, L.BN. Kier, A. Verloop and V. Pliska, *Int. J. Pept. Protein Res.*, **32**(4), 269 (1988).